Modeling host interactions with hepatitis B virus using primary and induced pluripotent stem cell-derived hepatocellular systems

Amir Shlomai[a,1], Robert E. Schwartz[b,c,1], Vyas Ramanan[c,1], Ankit Bhatta[a], Ype P. de Jong[a,d], Sangeeta N. Bhatia[b,c,e,f,g,h,2,3], and Charles M. Rice[a,2,3]

[a]Laboratory of Virology and Infectious Disease, Center for the Study of Hepatitis C, The Rockefeller University, New York, NY 10065; [b]Department of Medicine, Brigham and Women's Hospital, Boston, MA 02115; [c]Department of Health Sciences and Technology, [e]Department of Electrical Engineering and Computer Science, [g]Koch Institute for Integrative Cancer Research, and [h]Howard Hughes Medical Institute, Massachusetts Institute of Technology, Cambridge, MA 02139; [d]Division of Gastroenterology and Hepatology, Department of Medicine, Center for the Study of Hepatitis C, Weill Cornell Medical College, New York, NY 10065; and [f]Broad Institute of MIT and Harvard, Cambridge, MA 02139

Contributed by Charles M. Rice, July 10, 2014 (sent for review June 3, 2014)

Hepatitis B virus (HBV) chronically infects 400 million people worldwide and is a leading driver of end-stage liver disease and liver cancer. Research into the biology and treatment of HBV requires an in vitro cell-culture system that supports the infection of human hepatocytes, and accurately recapitulates virus–host interactions. Here, we report that micropatterned cocultures of primary human hepatocytes with stromal cells (MPCCs) reliably support productive HBV infection, and infection can be enhanced by blocking elements of the hepatocyte innate immune response associated with the induction of IFN-stimulated genes. MPCCs maintain prolonged, productive infection and represent a facile platform for studying virus–host interactions and for developing antiviral interventions. Hepatocytes obtained from different human donors vary dramatically in their permissiveness to HBV infection, suggesting that factors—such as divergence in genetic susceptibility to infection—may influence infection in vitro. To establish a complementary, renewable system on an isogenic background in which candidate genetics can be interrogated, we show that inducible pluripotent stem cells differentiated into hepatocyte-like cells (iHeps) support HBV infection that can also be enhanced by blocking interferon-stimulated gene induction. Notably, the emergence of the capacity to support HBV transcriptional activity and initial permissiveness for infection are marked by distinct stages of iHep differentiation, suggesting that infection of iHeps can be used both to study HBV, and conversely to assess the degree of iHep differentiation. Our work demonstrates the utility of these infectious systems for studying HBV biology and the virus' interactions with host hepatocyte genetics and physiology.

HBV persistence | innate immunity | viral hepatitis

Hepatitis B virus (HBV) is a small 3.2-kb DNA virus that selectively infects hepatocytes in the human liver (1). The global disease burden is large, with ∼400 million people chronically infected worldwide, of whom about one-third will develop severe HBV-related complications, such as cirrhosis and liver cancer. Lifelong treatment is often required because of the stable nature of viral episomal DNA, known as covalently closed circular DNA (cccDNA), which maintains basal levels in infected cell nuclei even upon nucleos(t)ide inhibitor treatment. To date, HBV research has been hampered by a distinct lack of robust infectious model systems that both support productive HBV infection and accurately mimic virus–host interactions. Recently, the bile acid pump sodium taurocholate cotransporting polypeptide (NTCP) has been identified as a receptor for both HBV and hepatitis D virus (2), and overexpression of NTCP in hepatoma cell lines renders them susceptible to HBV infection. However, hepatoma cells are known to be defective in many cellular pathways implicated in the innate immune response (3, 4), metabolism (5), and cell proliferation (6), which may contribute to published contradictory evidence regarding the extent to which HBV activates the innate immune response, and the importance of this response in curtailing infection (for a review, see ref. 7).

As the sole host cell infected by HBV in vivo, primary adult human hepatocytes represent the gold-standard for studying HBV interactions with the host. Prior studies have shown that primary human hepatocytes support HBV infection, although infection is usually not robust even upon supplementation of cell-culture medium with dimethyl sulfoxide (8) or polyethylene glycol (9). Moreover, primary human hepatocytes rapidly lose their hepatic phenotype shortly after isolation from the in vivo microenvironment (10, 11). We have previously developed a miniaturized system in which primary hepatocytes are organized in micropatterned colonies and surrounded by supportive stromal cells, providing hepatocytes with the necessary homotypic and heterotypic cell–cell interactions to promote long-term maintenance of their hepatic function (12). This micropatterned coculture (MPCC) system maintains hepatocyte phenotype and function over several weeks and has been shown to support robust infection with hepatitis C virus (HCV) and *Plasmodium*

Significance

Major obstacles for using human hepatocytes to study hepatitis B virus (HBV) pathobiology are rapid loss of hepatocyte function after plating and the variability between hepatocyte donors. We show that micropatterning and coculturing of primary human hepatocytes with fibroblasts (MPCC format) maintains prolonged infection that is restricted by the innate immune response, and can be further boosted by suppression of this response. To address the problem of donor variability, we show that induced pluripotent stem cells (iPSC) differentiated into hepatocyte-like cells support HBV infection in a differentiation-dependent manner. Our study opens an avenue for using these systems to study virus–host interactions and test antiviral drugs, and suggests HBV permissiveness as a surrogate reporter to assess the degree of differentiation of candidate iPSC-derived hepatocyte-like cells.

Author contributions: A.S., R.E.S., V.R., S.N.B., and C.M.R. designed research; A.S., R.E.S., V.R., A.B., and Y.P.d.J. performed research; A.S., R.E.S., V.R., A.B., S.N.B., and C.M.R. analyzed data; and A.S., R.E.S., V.R., S.N.B., and C.M.R. wrote the paper.

The authors declare no conflict of interest.

[1]A.S., R.E.S., and V.R. contributed equally to this work.

[2]S.N.B. and C.M.R. contributed equally to this work.

[3]To whom correspondence may be addressed. Email: ricec@rockefeller.edu or sbhatia@mit.edu.

This article contains supporting information online at www.pnas.org/lookup/suppl/doi:10.1073/pnas.1412631111/-/DCSupplemental.

MICROBIOLOGY

falciparum and *vivax* malaria (13, 14). We hypothesized that this system would be ideal for modeling HBV infection in vitro.

Beyond its potential utility for assessing virus–host interactions, studying the role of host factors in the MPCC system is complicated by limited availability and variability between donor hepatocytes. As a complementary approach that enables more facile genetic manipulation on an untransformed and isogenic hepatocyte background, we also sought to establish robust HBV infection in induced pluripotent stem cell (iPSC)-derived hepatocyte-like cells (iHeps) (15, 16). These cells have demonstrated their utility for modeling inherited metabolic disorders (17), incorporating genetic manipulations (18), and supporting infection with HCV (19–21). During iHep generation, the progression of differentiation is characterized by the sequential emergence of various hepatocyte-specific host factors known to play a role in the HBV life cycle, such as the transcription factor HNF4α and the nuclear receptor RXR (22). We show that permissiveness to HBV infection likewise progresses in a differentiation stage-specific manner. Thus, in this paper we use a system of stabilized primary hepatocytes for disease modeling to establish HBV infection in vitro and explore the use of directed differentiation of iPSCs to demonstrate that they serve as a suitable host population for the study of HBV and host–virus interactions.

Results

Micropatterned Human Hepatocytes Stably Express the HBV Receptor for Weeks in Culture. It has been hypothesized that primary human hepatocytes lose their permissiveness to HBV infection because of down-regulation of NTCP receptor expression upon isolation and subsequent culture (2). Our MPCCs of primary human hepatocytes and stromal fibroblasts (J2-3T3 fibroblasts, or J2s) maintain hepatocyte functions as well as polarity and promote the accurate localization of membrane proteins to hepatocytes' basolateral and apical domains (12). Although many distinct hepatocyte culture models have been explored in the literature, a telling control to probe the importance of tissue microarchitecture is seeding similar cellular constituents in a random configuration (random coculture, RCC) (Fig. 1*A*). NTCP was readily detected on the plasma membrane by immunostaining of hepatocytes in MPCCs (Fig. 1*B*), whereas the NTCP level at 18 d postplating was drastically reduced in RCCs (Fig. 1 *B–D*). Because viral spread is dependent upon consistent expression of the entry receptor, we analyzed NTCP levels over a course of 14 d, and found that NTCP protein and mRNA levels remained stable over time (Fig. S1*A*). These results establish the capacity of the MPCC format to maintain expression of the HBV receptor, NTCP, in vitro.

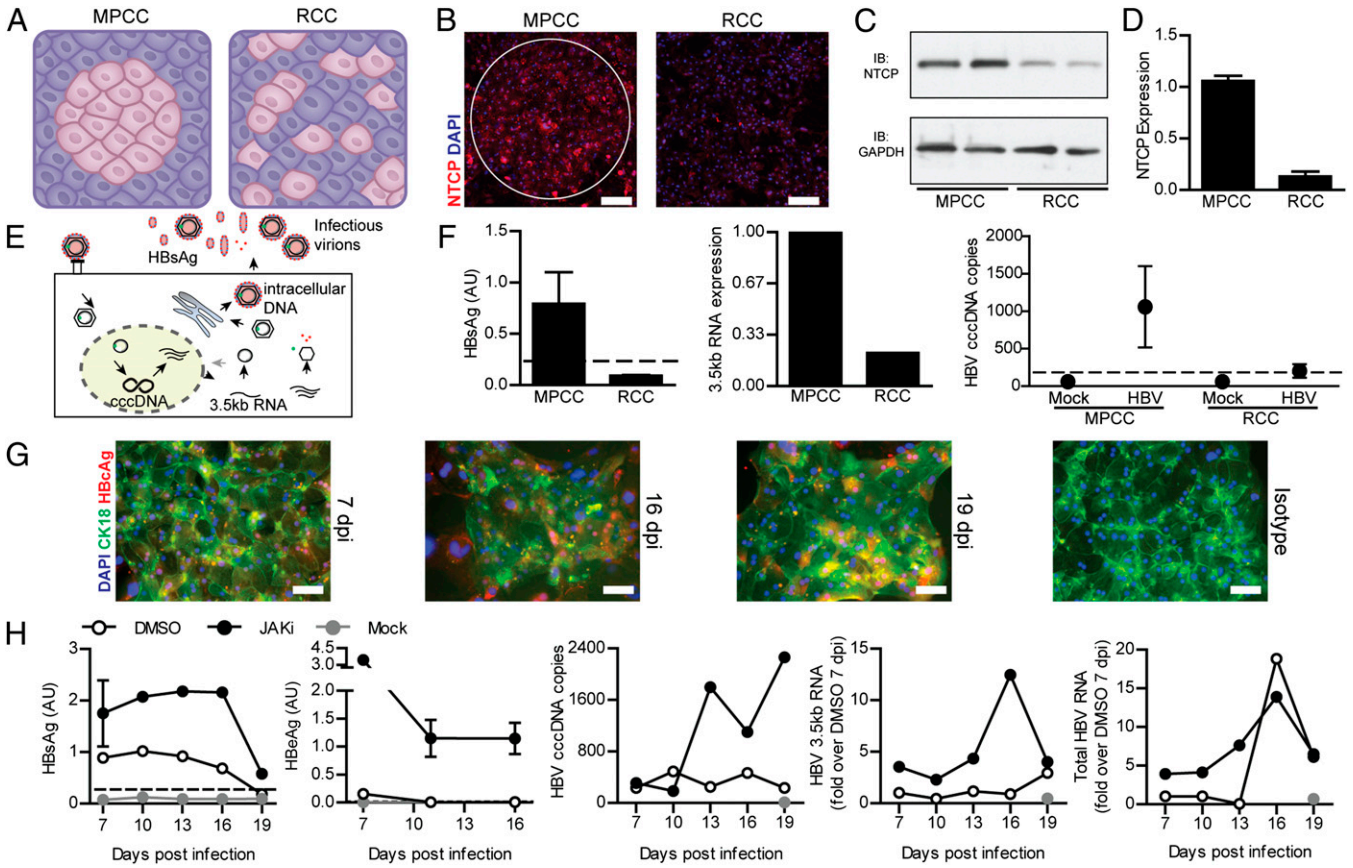

Fig. 1. HBV infection in micropatterned primary human hepatocytes is augmented by innate immune inhibition. (*A*) MPCC vs. RCC schematic. Hepatocytes in pink, fibroblasts in purple. (*B*) NTCP immunostaining: white circle marks hepatocyte island boundary. (Scale bar, 100 μm.) (*C*) NTCP Western blot. (*D*) NTCP quantitative RT-PCR (qRT-PCR; mean ± SEM, $n = 3$). (*E*) Schematic of viral life-cycle readouts used. (*F*, *Left*) ELISA for HBsAg, expressed as a mean ± SEM ($n = 3$), secreted into supernatant between 14 and 16 dpi; (*Center*) HBV 3.5-kb mRNA expression (one cell pellet per condition) at 16 dpi; (*Right*) Copies of cccDNA at 16 dpi, expressed as an average of biological duplicates ± range. (*G*) HBc immunostaining of MPCCs at the indicated days postinfection. Isotype-matched negative control shown. (Scale bars, 50 μm.) (*H*) Time course of HBV infection in MPCCs. (*Left* panels) HBsAg and HBeAg levels (average of triplicates) in supernatant; (*Center*) cccDNA levels; (*Right* panels) qRT-PCR for HBV 3.5-kb mRNA and total mRNA. Expression relative to DMSO-treated samples 7 dpi, one pellet per condition per experiment, verified across independent experiments. Dotted lines: limit of quantification (qPCR), cut-off (ELISA).

MPCCs Support Productive HBV Infection. Given the importance of the MPCC format for maintaining expression of the HBV receptor as well as other hepatocyte functions (Fig. S1 *B* and *C*), we next investigated whether MPCCs support HBV infection. We assayed various viral life-cycle stages, including viral gene expression, reflected by HBV surface antigen (HBsAg) secretion and 3.5-kb mRNA (the main HBV transcript) production, and the presence of the viral transcription template cccDNA, considered a hallmark of productive infection (Fig. 1*E*). We found that HBV derived from human infectious serum infects human hepatocytes more efficiently in MPCCs than RCCs (Fig. 1*F*). Furthermore, MPCCs support productive infection throughout the culture period of nearly 3 wk, based on immunostaining for HBV core (HBc) protein (Fig. 1*G*).

Based on previous data that the innate immune response can restrict HCV infection in hepatocytes (23), we explored pretreatment of MPCCs or RCCs with a broad-spectrum Janus kinase (JAK) inhibitor (JAKi), known to interfere with a major pathway of the innate immune axis by dampening expression of IFN-stimulated genes (ISGs) (24), in an attempt to elicit enhanced HBV replication efficiency. With the addition of JAKi, we observed more robust HBV infection in MPCCs (Fig. 1*H*) and detected cccDNA almost exclusively in this format (Fig. 1*F*, *Right*). Augmentation of HBV infection was also observed upon introduction of an inhibitor of TANK-binding kinase 1 (TBK1), an upstream activator of the IFN response pathway, although JAKi was more efficient in maintaining cccDNA following infection (Fig. S2). Collectively, these results suggest that the MPCC format supports the maintenance of productive infection over time in primary human hepatocytes, and that inhibition of major pathways of the hepatocyte innate immune response enhances infection in this system.

Temporal Expression of ISGs Following HBV Infection. In response to intracellular pathogen sensors, an innate immune pathway typically activates a set of ISGs, leading to autocrine/paracrine signaling by interferons. Based on our observation that addition of a JAK pathway inhibitor improved HBV infection in MPCCs, we hypothesized that the innate immune response may induce antiviral ISGs, at least in culture. To assay for this response, we incubated MPCCs with HBV infectious serum and analyzed the relative expression of type I IFNs, IFN-α, and IFN-β, as well as two genes implicated in type III IFN response, over the next 16 d (Fig. 2, *Left*). Both IFN-α and IFN-β were induced mainly late during the course of infection, although a modest induction (>two-fold) was detected as early as 12 h postinfection. The expression of a variety of ISGs implicated in antiviral responses were also detected following HBV infection, with a range of kinetic patterns, including several that function as sensors and transducers of these pathways (Fig. 2, *Center*), and a selection of antiviral effectors (Fig. 2, *Right*). Consistent with our hypothesis, we found that blunting the innate immune response with JAK inhibition blocked the expression of many downstream ISGs but had no significant effect on the expression of either IFN-α or IFN-β, which are regulated upstream of JAK-STAT signaling. We note that some exhibit a biphasic elevation over time, possibly representing reinfection events or expression in response to the emergence of later stage viral components. Importantly, ISG induction was dependent on productive HBV infection, because pretreatment of MPCCs with the HBV inhibitor entecavir largely abolished the induction of most early- and late-stage interferons and downstream ISGs (Fig. S3*A*).

Interestingly, although productive infection could be clearly detected in NTCP-expressing HepG2 hepatoma cells, as evidenced by production of HBV 3.5-kb mRNA (Fig. S3*B*, *Left*), no significant ISG induction was observed in these cells compared with HBV nonpermissive HepG2 cells (Fig. S3*B*, *Right*). These data suggest that either HBV sensors or key transducers in this sensing pathway are defective in hepatoma cells, highlighting a distinct opportunity of the MPCC system in terms of its potential for studying virus-host interactions in HBV infection.

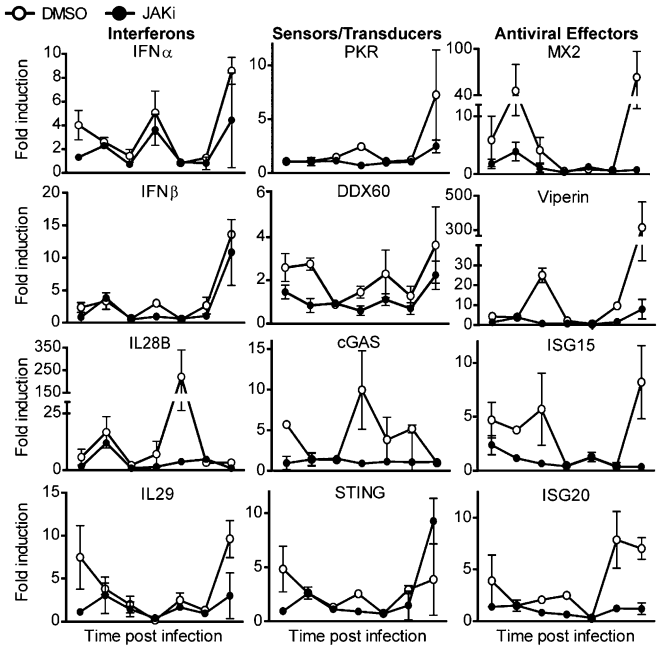

Fig. 2. Temporal induction of ISGs in HBV infected MPCCs. Primary human hepatocyte MPCCs were either mock- or HBV-infected with concomitant JAKi or DMSO (vehicle control) treatment. RNA expression was analyzed for the indicated ISGs at 12 h, 24 h, 48 h, 72 h, 7 d, 11 d, and 16 d postinfection and reported relative to the mock-infected cells, expressed as a mean ± SEM ($n = 3$).

MPCCs Offer the Potential to Study Antiviral Candidates. Following the demonstration that the MPCC format can support HBV infection, we asked whether the platform could be applied for use as an anti-HBV drug-testing tool. As proof-of-principle, we incubated MPCCs with HBV-infected serum with or without concomitant treatment with the HBV reverse-transcriptase inhibitor entecavir, or an alternate antiviral, IFN-β. The addition of prophylactic entecavir or IFN-β to MPCCs abrogated HBV infection, as indicated by a sharp decrease in the secretion of both HBV DNA and HBsAg into the medium over time (Fig. 3*A*). Consistent with these findings, levels of cellular 3.5-kb mRNA and cccDNA were also dramatically reduced in infected cells pretreated with IFN-β or with entecavir, as long as 21 d postinfection (dpi) (Fig. S4).

Having established that MPCCs can successfully model prophylactic drug protection against HBV, we assayed their potential utility to model a more clinically relevant regimen by starting treatment with IFN-β or entecavir 7 d after establishing HBV infection. Both treatments significantly reduced HBV DNA secretion into the medium by preinfected MPCCs, indicating an efficient inhibition of HBV replication (Fig. 3*B*). In contrast, only IFN-β, but not entecavir, abolished the levels of 3.5-kb mRNA and cccDNA observed at 16 dpi (9 d after initiating drug treatment), consistent with published differences in the capacity of reverse-transcriptase inhibitors versus interferons to promote cccDNA elimination (25). Collectively, these results demonstrate that the MPCC system can serve as a platform for studying the efficacy and mechanism of action of diverse antiviral agents, and has the potential to be expanded to a medium-to-high throughput drug-discovery tool (13, 26).

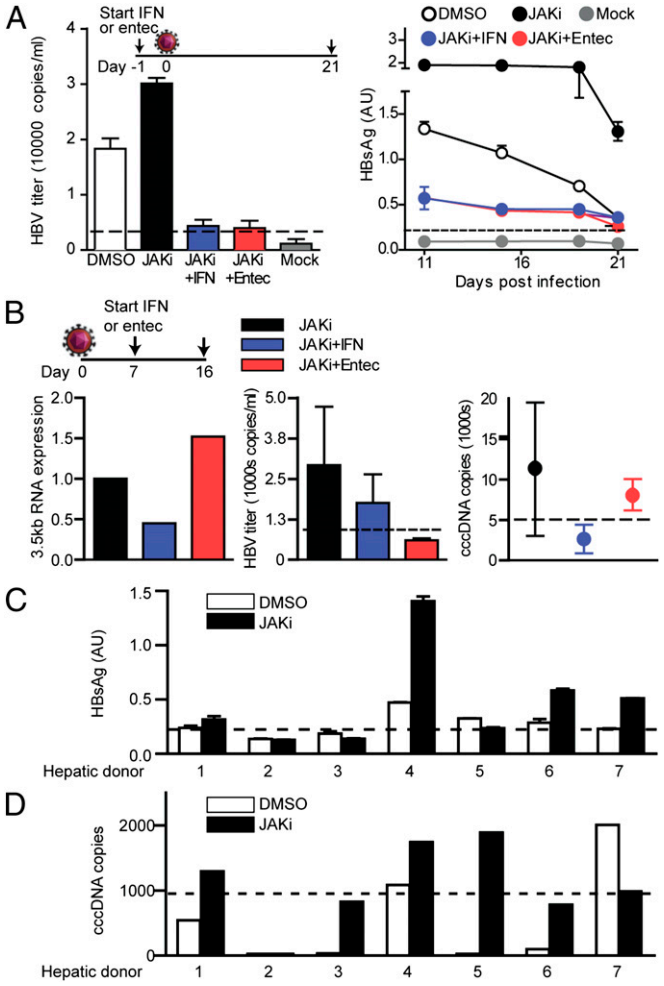

Fig. 3. MPCCs as a platform for anti-HBV drug studies. (*A*) MPCCs treated with DMSO or JAKi, with or without entecavir or IFN-β, were incubated with HBV infectious serum for 24 h, followed by continued drug treatment every 2 d. Collected supernatants were analyzed for HBV DNA after 3 wk (*Left*), and for secreted HBsAg at the indicated time points (*Right*); results are expressed as a mean ± SEM, $n = 3$. (*B*) HBV-infected MPCCs treated with JAKi were dosed with either IFN-β or entecavir from 7 to 16 dpi, when cell pellets were analyzed for 3.5-kb mRNA expression relative to nonantiviral treated cells (one cell pellet per condition, verified across multiple experiments; *Left*) and for cccDNA, expressed as an average (per cell pellet) of duplicates ± range (*Right*). Also at 16 dpi, medium (last changed at 14 dpi) was analyzed for secreted HBV DNA, expressed as a mean ± SEM ($n = 3$) (*Center*). (*C* and *D*) JAKi or DMSO-treated MPCCs bearing primary human hepatocytes from different donors were incubated with HBV infectious serum and assayed at 16 dpi for HBsAg, expressed as average of duplicates, and cccDNA quantification, total copies per cell pellet. Dotted lines indicate limit of quantification (qPCR) or cut-off (ELISA).

Hepatic Donors That Share a Differentiated Phenotype in Vitro Exhibit Variable HBV Permissiveness. To establish a viable drug testing platform, it is essential to identify a source of reproducibly infectible hepatocytes. The advent of cryopreserved human hepatocytes partially achieves this goal, in terms of offering a uniform donor source. To examine the importance of host variability in HBV infection of MPCCs, we used MPCCs seeded with hepatocytes derived from different hepatic donors (HD) (Table S1) and incubated them with patient-derived HBV infectious serum. Analyzing markers of productive infection revealed a wide variation between donors, with hepatic donor 4 (HD4) showing the most robust HBsAg production (Fig. 3*C*) and cccDNA formation (Fig. 3*D*). Notably, blocking the type I IFN response by treating the cells with JAK inhibitor generally resulted in increased HBsAg secretion, as well as cccDNA production, although in some donors (such as HD2), even JAK inhibition was unable to promote the production of detectable levels of cccDNA. Furthermore, the interdonor variation in infection levels did not correlate with other established biomarkers of hepatocyte function (Fig. S5). Collectively, these results suggest that MPCCs support HBV infection in a hepatocyte donor-dependent manner. Although technical factors implicated in hepatocyte isolation and cryopreservation may play a role, it is also possible that a divergence in genetically determined host factors may underlie this variation.

iPSC-Derived iHeps as a Candidate HBV Host in Vitro. To overcome the variability in HBV permissiveness observed among donors of primary human hepatocytes, we considered options for generating a physiologically relevant in vitro system on an isogenic background. iPSCs are renewable, can be derived from a single donor, and repeatedly differentiated into iHeps that share features of human hepatocytes (15, 16, 26) (Fig. S6*A*). To ascertain whether iHeps might be permissive to HBV infection, we first investigated the expression kinetics of NTCP during the course of iHep differentiation. Using immunostaining, we observed that although NTCP was barely detectable on day 15, it was readily detectable 3 d later and increased throughout the remainder of the differentiation protocol (Fig. S6*B*, *Left*). Consistent with the protein-expression findings, quantitative analysis of NTCP mRNA levels also showed a gradual increase throughout differentiation, although the level achieved in day 20 differentiated iHeps remained less than that observed in cryopreserved primary adult hepatocytes (Fig. S6*B*, *Right*).

In addition to the dependence on an entry receptor, iHeps must also exhibit the capacity to support HBV transcription to support replication. Thus, we assessed the earliest stage at which differentiating iHeps achieved this milestone by transfecting them with an HBV luciferase reporter construct (Fig. S6*C*). Although the liver-enriched transcription factor HNF-4α, central to the activation of the HBV transcriptional program (27), is expressed early during iHep differentiation (22, 28) (Fig. S6*A*), HBV transcriptional activity was not detected until day 18, after which it continued to rise (Fig. S6*C*).

iHeps Support Productive HBV Infection During Late Stages of Differentiation. To investigate whether iPSC-derived iHeps are permissive to productive HBV infection, we incubated differentiating iPSCs with HBV infectious serum and assayed for markers of the viral life cycle. Analysis performed at 16 dpi revealed signs of productive infection in fully differentiated iHeps (day 20 of differentiation), but not in cells infected at earlier stages of differentiation, as evidenced by 3.5-kb mRNA expression, HBsAg secretion, and cccDNA accumulation (Fig. 4 *A*–*C*). To examine both the specificity and kinetics of HBV infection of day 20 iHeps, we incubated cells with HBV infectious serum with or without JAKi and the antiviral drug entecavir. When analyzed over a 3-wk period, only JAKi-treated iHeps maintained significant secretion of HBsAg over time, in contrast to a rapid loss of HBsAg produced by vehicle-treated or entecavir-treated cells (Fig. 4*D*). However, HBV DNA, both quantified (Fig. S7) and also analyzed by Southern blot (showing mainly relaxed circular replicative forms migrating at around 3.2 kb) (Fig. 4*E*), as well as HBV core protein (Fig. 4*F*) were detected in day 20 iHeps, largely independent of JAK inhibition. Given this discrepancy, we analyzed the effect of HBV infection on innate immune activation in iHeps, where we detected induction of many of the same ISGs that were observed in HBV-infected MPCCs (Fig. 4*G*). However, most of the ISG transcripts produced by infected iHeps were rarely elevated to the same magnitude, with the exception of viperin, which was induced over 15-fold in day 20 iHeps, relative to day 7 iHeps, which were

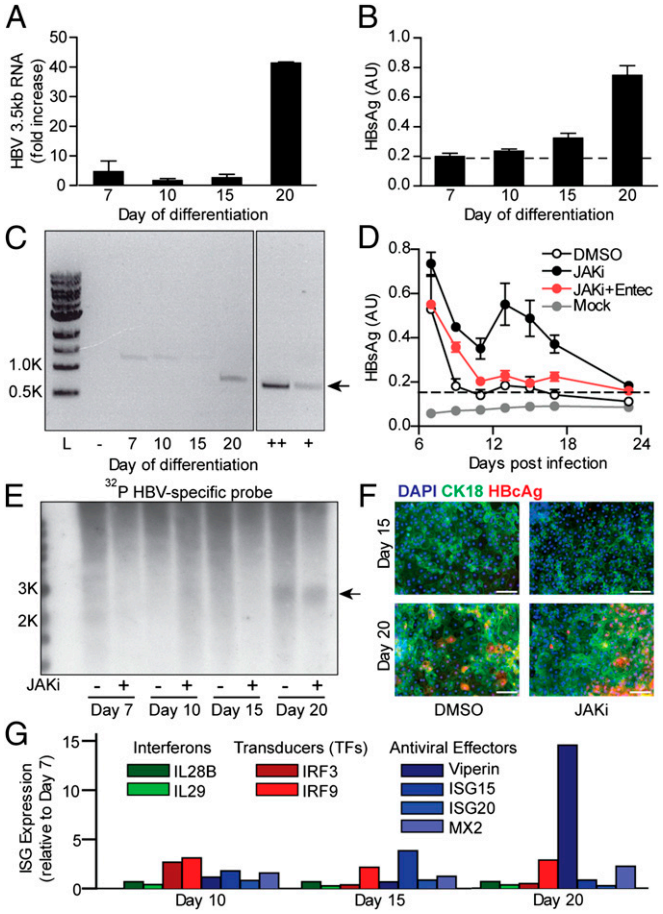

Fig. 4. HBV infection of iHeps is drug-sensitive and differentiation-dependent. (*A–C*) iPSCs were differentiated in a stepwise fashion, treated with JAKi and incubated with HBV infectious serum upon treatment at the indicated days of the differentiation protocol. (*A*) At 16 dpi, HBV 3.5-kb mRNA was quantified by qRT-PCR, shown relative to DMSO-treated cells infected at day 10 of differentiation, and expressed as the mean ± SEM across two separate experiments. (*B*) Also at 16 dpi, medium (last changed at 14 dpi) was analyzed for secreted HBsAg (mean ± SEM, $n = 3$). (*C*) Agarose gel separation of amplified cccDNA products (16 dpi) on a single gel with high- (++) and low- (+) expression positive controls (size mismatch because of slight curvature between distant lanes). (*D*) Differentiated iHeps (day 20 of differentiation) treated as indicated were incubated with HBV infectious serum, followed by HBsAg measurements in media, expressed as a mean ± SEM ($n = 3$). (*E* and *F*). iPSCs were incubated with HBV infectious serum at the indicated days of differentiation with DMSO or JAKi. (*E*) Southern blot of cellular DNA extracted at 16 dpi (*SI Materials and Methods*) using an HBV-specific probe; arrow indicates bands corresponding to HBV DNA (predicted to be relaxed, circular DNA at this size). (*F*) HBcAg immunofluorescent staining of DMSO- or JAKi-treated 16-dpi iPSCs infected at day 15 and 20 of differentiation; (Scale bar, 50 μm.) (*G*) ISG mRNA expression by qRT-PCR of HBV-infected iHeps at 16 dpi, normalized to the expression of HBV infected cells at day 7 of differentiation.

essentially uninfected by HBV. Collectively, these results suggest that iPSCs at advanced stages of the hepatic differentiation program support productive HBV infection, which can be maintained over a period of weeks with the addition of an innate immune response inhibitor.

Discussion

In this study, we report HBV infection in two complementary patient-derived hepatocyte systems in which infection is limited by an innate immune response, and demonstrate the utility of these systems for studying virus–host interactions. The establishment of two complementary HBV model systems represents an opportunity to tackle questions regarding major components of the viral entry process and viral life cycle, including host factors underlying establishment and persistence of a nuclear cccDNA pool, the key viral reservoir that leaves patients susceptible to viral reactivation (29).

The MPCC system uses micropatterned primary human hepatocytes cocultured with stromal fibroblasts, a format that ensures the prolonged viability and functionality of these delicate cells (12). By comparing the HBV permissiveness of MPCCs to that of cocultured cells seeded in a random format, we show that the patterning provided by the MPCC format is essential to maintaining productive infection for up to 3 wk. An advantage of the MPCC system is its facility for interrogating the identity of host factors responsible for the observed permissiveness, in that cryopreserved donor cells that exhibit comparable hepatocyte functions in culture but disparate permissiveness to HBV infection can be subjected to systematic molecular analysis. In this manner, candidate host-factor pathways and drug-targeting strategies may be explored in vitro.

We can also leverage inherent strengths of the iHep system to identify candidate essential host factors that confer HBV sensitivity. In the differentiating populations, we observe that HBV transcriptional activity increases over time, and can be overlaid with the stepwise process of hepatocyte-specific factor acquisition. Thus far, our differentiation time-course data tracking both NTCP expression and HBV promoter/enhancer element-driven luciferase expression demonstrate that the up-regulation of both entry factors and other transcription-related host factors are essential for successful infection by HBV. We observe a tipping point for permissiveness at around days 18–20 of the iHep differentiation process, corresponding to a switch from a hepatoblast-like phenotype to one resembling fetal hepatocytes. A comparison of populations on either side of this time point may identify candidate pathways, to be filtered based on findings from the MPCC system, and interrogated via directed mutagenesis or selective generation of iPSC lines from desired genotypes. In addition, the stage-specific acquisition of permissiveness to hepatotropic pathogens may offer a novel method for assessing the relative success of candidate in vitro differentiation protocols.

One important suite of host factors consists of the proteins involved in the hepatocyte innate immune response, the role of which in restricting HBV infection has been difficult to pin down (7). Much of this debate has resulted from deficiencies in the model systems used for HBV studies, because commonly used hepatoma cell lines possess well-documented defects in innate immune sensing and signal transduction (3, 4). In our systems, the establishment of productive and long-lasting infection was aided by inhibiting the innate immune response with inhibitors of the JAK family or the signaling intermediate TBK1. However, our data show that JAK inhibition boosted infection much more in MPCCs than in day 20 differentiated iHeps, as evidenced by the similar levels of viral replication achieved with and without JAK inhibition in differentiated iHeps (Fig. 4). This difference may be caused by the weaker induction of ISGs observed in HBV-infected iHeps compared with MPCCs, reflecting differences in host innate immune response between fully differentiated primary human hepatocytes and iPSC-induced hepatocyte-like cells (30, 31). Still, the differential effect of JAK inhibition on different markers of viral replication (e.g., large effects on HBsAg secretion but minor effects on replicative intermediate formation) observed in iHeps is not entirely clear and requires further study.

Our observation that innate immune activation restricts HBV infection is consistent with studies showing that HBV can be cleared from the liver in a cytokine-mediated, noncytotoxic manner (25, 32), and that HBV replication is significantly reduced in chimpanzees chronically infected with HCV because of the induction of the type I IFN response (33). In contrast to the robust induction of ISGs in HBV-infected MPCCs, and to a lesser extent in iHeps, no ISG response was observed in HBV-permissive

HepG2 cells overexpressing NTCP. This finding emphasizes the advantage of both MPCCs and iHeps over hepatoma cell lines and traditional hepatocyte culture systems in the analysis of virus–host interactions, in particular innate immune responses. A similar induction of the type I IFN response accompanied by up-regulation of ISGs was previously observed in HBV-permissive HepaRG cells, but not in HepG2 cells upon induction of a baculovirus expressing HBV (34). However, even in HepaRG cells, the bipotential nature of the cells suggests an immature state in which the innate immune axis may not be fully developed. Similarly, our observation that iHeps display more modest, differentiation stage-dependent ISG induction relative to MPCCs, may be explained by the finding that the innate immune axis matures in concert with the hepatic phenotype of differentiating iHeps (35). Thus, our results support the model that the innate immune system plays a role in HBV infection and suggests that HBV may be less of a "stealth virus" than previously thought (36).

Notably, in the MPCC platform, we observed that a constant fraction of around 25% of the cells were HBc-positive between 7 and 19 d postinfection. This absence of apparent viral spread raises the possibility that viral production is not robust enough to support reinfection, or that the rate of new infection is offset by viral clearance from other cells. In addition, given the prolonged maintenance of normal hepatocyte function in the MPCC system, it is not clear why levels of HBV surface antigen and DNA secretion drop precipitously by 21 dpi. One possible explanation is that a gradual reduction in host factors essential to the viral transcription/replication machinery induces an eventual block at the level of gene expression or replication. The observation that the cccDNA level remains relatively stable even after the sharp decline in the viral gene expression and replication raises the intriguing possibility that these kinetics represent a switch from a more acute stage of infection to one that is more chronic and low-level.

In summary, we show that MPCCs and pluripotent stem cell-derived iHeps are both permissive to and support productive HBV infection. We envision these platforms to be complementary, each with their own advantages, and also each with the capacity to inform further optimization of the other. Thus, the combination of our HBV infectious systems will open new avenues to more fully characterize the HBV life cycle and its interaction with the host, thereby promoting the identification of potential drug targets for a disease infecting 400 million people globally.

Materials and Methods

The experimental conditions used to generate MPCCs, maintain iPSCs, and differentiate iHeps have all been previously described (12, 15, 16, 19). For HBV infection of MPCCs and iHeps, cultures were pretreated for 24 h with dimethyl sulfoxide [0.01% (vol/vol)], JAKi (1 μM; EMD Millipore), TBK1 inhibitor (1 μM; EMD Millipore), IFN-β (1,000 U/mL; R&D Systems), or entecavir (120 nM; Cayman Chemicals), as indicated, followed by infection with HBV^+ patient plasma. Additional details are described in *SI Materials and Methods*, including techniques used to assess HBV infection, such as total DNA, cccDNA, RNA analysis, immunofluorescence, and ELISA for HBsAg and HBeAg.

ACKNOWLEDGMENTS. We thank H. Fleming for manuscript editing. This study was supported in part by The Center for Basic and Translational Research on Disorders of the Digestive System through the generosity of the Leona M. and Harry B. Helmsley Charitable Trust (A.S.), Skolkovo Institute of Science and Technology Grant 022423-003 (to S.N.B.), National Institutes of Health Grants UH2 EB017103 (to S.N.B.) and DK085713 (to C.M.R. and S.N.B.), the Koch Institute Support Grant P30-CA14051 from the National Cancer Institute (Swanson Biotechnology Center), an American Gastroenterology Association Research Scholar Award and National Institutes of Health Grant 1K08DK101754 (to R.E.S.), and a Fannie and John Hertz Foundation fellowship and National Science Foundation Graduate Research fellowship (to V.R.). A.S. is a trainee at the Clinical Scholar Program, The Rockefeller University, supported by Grant 8 UL1 TR000043 from the National Center for Research Resources and the National Center for Advancing Translational Sciences, National Institutes of Health. S.N.B. is a Howard Hughes Medical Institute Investigator.

1. Ganem D, Varmus HE (1987) The molecular biology of the hepatitis B viruses. *Annu Rev Biochem* 56:651–693.
2. Yan H, et al. (2012) Sodium taurocholate cotransporting polypeptide is a functional receptor for human hepatitis B and D virus. *eLife* 1:e00049.
3. Li K, Chen Z, Kato N, Gale M, Jr, Lemon SM (2005) Distinct poly(I-C) and virus-activated signaling pathways leading to interferon-β production in hepatocytes. *J Biol Chem* 280(17):16739–16747.
4. Tnani M, Bayard BA (1999) Evidence for IRF-1-dependent gene expression deficiency in interferon unresponsive HepG2 cells. *Biochimica et Biophysica Acta* 1451(1):59–72.
5. Lu H, Forbes RA, Verma A (2002) Hypoxia-inducible factor 1 activation by aerobic glycolysis implicates the Warburg effect in carcinogenesis. *J Biol Chem* 277(26): 23111–23115.
6. Tsukada Y, Miyazawa K, Kitamura N (2001) High intensity ERK signal mediates hepatocyte growth factor-induced proliferation inhibition of the human hepatocellular carcinoma cell line HepG2. *J Biol Chem* 276(44):40968–40976.
7. Bertoletti A, Ferrari C (2012) Innate and adaptive immune responses in chronic hepatitis B virus infections: Towards restoration of immune control of viral infection. *Gut* 61(12):1754–1764.
8. Gripon P, et al. (1988) Hepatitis B virus infection of adult human hepatocytes cultured in the presence of dimethyl sulfoxide. *J Virol* 62(11):4136–4143.
9. Gripon P, Diot C, Guguen-Guillouzo C (1993) Reproducible high level infection of cultured adult human hepatocytes by hepatitis B virus: Effect of polyethylene glycol on adsorption and penetration. *Virology* 192(2):534–540.
10. Guillouzo A (1998) Liver cell models in in vitro toxicology. *Environ Health Perspect* 106(Suppl 2):511–532.
11. Hewitt NJ, et al. (2007) Primary hepatocytes: Current understanding of the regulation of metabolic enzymes and transporter proteins, and pharmaceutical practice for the use of hepatocytes in metabolism, enzyme induction, transporter, clearance, and hepatotoxicity studies. *Drug Metab Rev* 39(1):159–234.
12. Khetani SR, Bhatia SN (2008) Microscale culture of human liver cells for drug development. *Nat Biotechnol* 26(1):120–126.
13. March S, et al. (2013) A microscale human liver platform that supports the hepatic stages of *Plasmodium falciparum* and *vivax*. *Cell Host Microbe* 14(1):104–115.
14. Ploss A, et al. (2010) Persistent hepatitis C virus infection in microscale primary human hepatocyte cultures. *Proc Natl Acad Sci USA* 107(7):3141–3145.
15. Schwartz RE, Fleming HE, Khetani SR, Bhatia SN (2014) Pluripotent stem cell-derived hepatocyte-like cells. *Biotechnol Adv* 32(2):504–513.
16. Si-Tayeb K, et al. (2010) Highly efficient generation of human hepatocyte-like cells from induced pluripotent stem cells. *Hepatology* 51(1):297–305.
17. Rashid ST, et al. (2010) Modeling inherited metabolic disorders of the liver using human induced pluripotent stem cells. *J Clin Invest* 120(9):3127–3136.
18. Yusa K, et al. (2011) Targeted gene correction of α1-antitrypsin deficiency in induced pluripotent stem cells. *Nature* 478(7369):391–394.
19. Schwartz RE, et al. (2012) Modeling hepatitis C virus infection using human induced pluripotent stem cells. *Proc Natl Acad Sci USA* 109(7):2544–2548.
20. Wu X, et al. (2012) Productive hepatitis C virus infection of stem cell-derived hepatocytes reveals a critical transition to viral permissiveness during differentiation. *PLoS Pathog* 8(4):e1002617.
21. Roelandt P, et al. (2012) Human pluripotent stem cell-derived hepatocytes support complete replication of hepatitis C virus. *J Hepatol* 57(2):246–251.
22. DeLaForest A, et al. (2011) HNF4A is essential for specification of hepatic progenitors from human pluripotent stem cells. *Development* 138(19):4143–4153.
23. Andrus L, et al. (2011) Expression of paramyxovirus V proteins promotes replication and spread of hepatitis C virus in cultures of primary human fetal liver cells. *Hepatology* 54(6):1901–1912.
24. Schneider WM, Chevillotte MD, Rice CM (2014) Interferon-stimulated genes: A complex web of host defenses. *Annu Rev Immunol* 32(1):513–545.
25. Lucifora J, et al. (2014) Specific and nonhepatotoxic degradation of nuclear hepatitis B virus cccDNA. *Science* 343(6176):1221–1228.
26. Shan J, et al. (2013) Identification of small molecules for human hepatocyte expansion and iPS differentiation. *Nat Chem Biol* 9(8):514–520.
27. Li L, et al. (2009) Developmental regulation of hepatitis B virus biosynthesis by hepatocyte nuclear factor 4α. *PLoS ONE* 4(5):e5489.
28. Li J, Ning G, Duncan SA (2000) Mammalian hepatocyte differentiation requires the transcription factor HNF-4α. *Genes Dev* 14(4):464–474.
29. Dandri M, Locarnini S (2012) New insight in the pathobiology of hepatitis B virus infection. *Gut* 61(Suppl 1):i6–i17.
30. Burke DC, Graham CF, Lehman JM (1978) Appearance of interferon inducibility and sensitivity during differentiation of murine teratocarcinoma cells in vitro. *Cell* 13(2): 243–248.
31. Pare JM, Sullivan CS (2014) Distinct antiviral responses in pluripotent versus differentiated cells. *PLoS Pathog* 10(2):e1003865.
32. Guidotti LG, et al. (1999) Viral clearance without destruction of infected cells during acute HBV infection. *Science* 284(5415):825–829.
33. Wieland SF, Asabe S, Engle RE, Purcell RH, Chisari FV (2014) Limited hepatitis B virus replication space in the chronically hepatitis C virus-infected liver. *J Virol* 88(9):5184–5188.
34. Lucifora J, et al. (2010) Control of hepatitis B virus replication by innate response of HepaRG cells. *Hepatology* 51(1):63–72.
35. Zhu S, et al. (2014) Mouse liver repopulation with hepatocytes generated from human fibroblasts. *Nature* 508(7494):93–97.
36. Durantel D, Zoulim F (2009) Innate response to hepatitis B virus infection: Observations challenging the concept of a stealth virus. *Hepatology* 50(6):1692–1695.

Supporting Information

Shlomai et al. 10.1073/pnas.1412631111

SI Materials and Methods

Primary Human Adult Hepatocytes. Primary human hepatocytes were purchased from vendors permitted to sell products derived from human organs procured in the United States by federally designated Organ Procurement Organizations. Vendors included: Celsis In Vitro Technologies (Celsis), Triangle Research Labs (TRL), and VWR through Xenotech (VWR) (See Table S1). Human hepatocytes were pelleted by centrifugation at 50–100 × *g* for 5–10 min at 4 °C, resuspended in hepatocyte culture medium, and assessed for viability using trypan blue exclusion (typically 70–90%).

Inducible Pluripotent Stem Cell Culture and Induced Hepatocyte-Like Cell Generation. In brief, inducible pluripotent stem cells (iPSCs) were cultured in monolayers on matrigel (Becton Dickinson), and directed differentiation was achieved by sequential exposure to activin A (R&D Systems), bone morphogenic protein 4 (R&D Systems), basic fibroblast growth factor (Invitrogen), hepatocyte growth factor (R&D Systems), and oncostatin M (R&D Systems) (1).

Micropatterned Cocultures. Off-the-shelf tissue-culture polystyrene (24-) or glass-bottom (24-) multiwell plates, coated homogenously with rat tail type I collagen (50 μg/mL), were subjected to soft-lithographic techniques to pattern the collagen into microdomains (islands of 500 μm in diameter with 900-μm center-to-center spacing). To create micropatterned cocultures (MPCCs), cryopreserved adult human hepatocytes were seeded on collagen-patterned plates that mediate selective cell adhesion. The cells were washed with medium 2–3 h later (~4×10^4 adherent hepatocytes in 96 collagen-coated islands in a 24-well plate) and incubated in hepatocyte medium overnight. Hepatocyte culture medium was DMEM with high glucose, 10% (vol/vol) FBS, 1% (vol/vol) ITS premix (BD Biosciences, cat No 354352), 7 ng/mL glucagon, 40 ng/mL dexamethasone, and 1% penicillin-streptomycin. 3T3-J2 murine embryonic fibroblasts were seeded (9×10^4 cells in each well of a 24-well plate) 24-h later. Hepatocyte culture medium was replaced 24 h after fibroblast seeding and subsequently replaced every other day. Randomly cultured cocultures (RCCs) of hepatocytes and 3T3-J2 fibroblasts were created as described previously (2). Briefly, RCCs were generated by seeding 2×10^5 hepatocytes per well of a collagen-coated 24-well plate, followed by addition of 9×10^4 J2-3T3 cells the next day, all in the same hepatocyte culture medium as used in MPCCs. There is a fivefold increase in hepatocytes per well in RCCs compared with MPCCs, but these numbers were chosen because hepatocyte survival is improved in denser culture.

Hepatitis B Virus Infection of MPCCs and Induced Hepatocyte-Like Cells. The concentration of entecavir was chosen as 30× the EC_{50} according to the literature (3). De-identified plasma positive for hepatitis B virus (HBV) but negative for HCV and HIV was obtained from the Red Cross. For all of the experiments presented in this study, three stocks of plasma derived from three different donors were used. Two stocks were genotype D the other genotype A. Genotypes were determined using DNA extracted from plasma by PCR using primers (F) 5′-CTCCACCAATCGGCAGTC-3′ and (R) 5′-AGTCCAAGAGTCCTCTTATGTAAGACCTT-3′. PCR products were sequenced using the following primer: 5′-CCTCTGCCGATCCATACTGCGGAAC-3′ and genotypes were determined using the National Center for Biotechnology Information genotyping online tool (www.ncbi.nlm.nih.gov/projects/genotyping/formpage.cgi). For infection, calcium chloride was added to the plasma at a final concentration of 1.25 mM and incubated for 30 min at 37 °C. The gelled plasma was then spun at 14,000 × *g* for 5 min, and the prior two steps repeated until no gelled clots remained. The supernatant remaining (serum) was then used to inoculate MPCC or induced hepatocyte-like cells (iHeps) at a 1:10–1:20 dilution in standard culture medium for 24 h. The calculated multiplicity of infection, based on initial viral (DNA) titer and cell number, was between 300 and 350 HBV genomes per cell. Cells were washed five times with DMEM, then new hepatocyte culture media or iHep culture media was added. Every 48 h, medium was collected and stored at −80 °C for subsequent analyses and replaced with fresh medium.

Quantification of Intracellular or Secreted HBV DNA in iPSC-Derived and Primary Hepatocytes. Cell pellets or media were collected and DNA was extracted using the QIAamp DNA blood mini kit (QIAGEN, cat No 51104) or QIAamp Minielute Virus spin kit (QIAGEN, cat No 57704), respectively. DNA was extracted according to the manufacturer's protocol, and the final product was eluted in 60 μL of water. Five microliters was taken for a quantitative PCR (qPCR).

Quantification of Total HBV DNA. qPCR for HBV DNA was performed using the TaqMan Universal PCR Master Mix (Applied Bio systems, cat No 4304437) and the following primers and probe: 5′-CCGTCTGTGCCTTCTCATCTG-3′ (sense), 5′-AGTCCAAGAGTCCTCTTATGTAAGACCTT-3′ (antisense), 5- /56-FAM/CCG TGT GCA /ZEN/CTT CGCTTC ACCTCT GC/ 3IABkFQ/ -3 (probe). PCR was performed using the Roche LightCycler 480 and the following conditions: (*i*) denaturation at 50 °C for 5 min followed by 95 °C for 10 min (one cycle); (*ii*) qPCR at 95 °C for 15 s, 56 °C for 40 s, and 72 °C for 20 s (40 cycles); (*iii*) melting at 65 °C for 10 s, followed by 95 °C (continuous).

Quantification was done by using a standard curve composed from 2× HBV plasmid over a range of 10^9–10^1 copies.

HBV Covalently Closed Circular DNA Quantification. DNA extracted from cells was subjected to overnight digestion with a plasmid-safe DNase (Epicentre), as previously described (4). Following enzyme inactivation at 70 °C for 30 min, DNA was subjected to real-time PCR using SYBR Premix Ex Taq (TaKaRa) following a protocol previously described (4) and using the covalently closed circular DNA (cccDNA) -specific primers described by Glebe et al. (5).

The primers used for cccDNA amplification were 5′-TGCACTTCGCTTCACCTF-3′ (sense), 5′-AGGGGCATTTGGTGGTC-3′ (antisense). For quantification, a standard curve derived from decreasing concentrations of 2× HBV plasmid was used.

PCR was performed using the Roche LightCycler 480 and the following conditions: (*i*) denaturation at 95 °C for 2 min (one cycle); (*ii*) qPCR at 95 °C for 10 s, 63 °C for 20 s, and 72 °C for 45 s (40 cycles); (*iii*) melting at 95 °C for 10 s, 65 °C for 10 s, and 95 °C (continuous).

Analysis of HBV DNA Forms. Total DNA was extracted using the QIAamp DNA blood mini kit (QIAGEN, cat No 51104) in a procedure involving cell lysis and proteinase K treatment (without prior DNaseI treatment). Total DNA was later run on 0.8% agarose-TAE gel, followed by denaturation and Southern blotting to a Hybond N nylon membrane (Amersham). Viral DNA was detected by hybridization with a ^{32}P random primed HBV probe, using the Prime-It II Random Primer Labeling Kit (Agilent

Technologies, Cat No 300385). Following incubation and washing, hybridized species were visualized by phosphorimaging and film exposure.

Analysis of Viral and Cellular mRNAs in MPCC and iPSC-Derived iHeps. Total RNA was isolated with the RNeasy Plus Mini Kit (Qiagen) or via TRIZOL RNA/DNA extraction. RNA was quantified using a NanoDrop, and first-strand cDNA was synthesized using Moloney murine leukemia virus RT (Bio-Rad) or SuperScript III RT kit (Invitrogen). qPCR for various genes/mRNAs including HBV 3.5 kb and total transcripts, IFN-stimulated genes, bile acid pump sodium taurocholate cotransporting polypeptide (NTCP), and differentiation factors was carried out with Taq polymerase and SYBR Green in the supplier's reaction buffer containing 1.5 mM $MgCl_2$ (Bio-Rad). For amplification of HBV 3.5-kb mRNA or total HBV mRNAs, we used primers spanning the 5′ end common only to the HBV long transcript or the region upstream to the poly(A) signal spanning the 3′ of all mRNAs, respectively, as previously described (4). To rule out HBV DNA contamination, total RNA was pretreated with DNaseI before first-strand synthesis and for every qRT-PCR analysis, a negative control (without reverse transcriptase) was included. qRT-PCR results for HBV transcripts were normalized to the human RPS11 housekeeping gene; other qRT-PCR results were normalized to β-actin (and verified with GAPDH). Oligonucleotide primer sequences are available by request. Amplicons were analyzed by 2% (wt/vol) agarose gel electrophoresis (Bio-Rad).

Detection of Secreted Hepatitis B Surface Antigen. One-hundred microliters of medium was loaded on ELISA plates coated with mouse monoclonal anti-hepatitis B surface antigen (HBsAg) antibodies (Bio-Rad, GS HBsAg EIA 3.0, Cat. No. 32591). ELISA was carried out according to the manufacturer's instructions. Plates were read using the FLUOstar Omega luminometer (BMG LABTECH). HBsAg positivity (cut-off) was calculated as an average of three negative controls + 0.07 (this value was optimized to avoid false–positive identification of HBsAg).

Detection of Secreted Hepatitis B e-Antigen. Fifty microliters of medium was loaded on ELISA plates coated with mouse monoclonal anti-hepatitis B e-antigen (HBeAg) antibodies (AbNova KA3288). ELISA was performed according to the manufacturer's instructions using HRP detection with 3,3′,5,5′-tetramethylbenzidine (Thermo Scientific) substrate.

HBV Transcription During iHep Differentiation. For HBV transcription during iHep differentiation, 1.3 × HBV-Luc, in which a luciferase cassette is cloned downstream of the EnhII and pre-C/C promoter, was a kind gift from Y. Shaul (The Weizmann Institute, Rehovot, Israel) (6). Ten micrograms of HBV-Luc plasmid DNA was transfected using TransIT-2020 reagent (Mirus) to 1.0×10^6 iPSC/iHeps at varying stages of differentiation. Cells were analyzed 72–96 h posttransfection for luciferase expression. Briefly, cells were incubated with D-luciferin (Invitrogen) for 10 min and then imaged using an IVIS Spectrum optical imaging system. Bioluminescent images were acquired using the autoexposure function. Data analyses for signal intensities and image comparisons were performed using Living Image software (Caliper Life Sciences). To calculate radiance for each well, the well size was delinated and each signal was expressed as radiance (photons per s/cm^2 per steradian). To rule out variations in transfection efficiency, cells were cotransfected with a GFP-expressing plasmid and GFP$^+$ cells quantified by fluorescence microscopy 72 h posttransfection. In addition, intracellular DNA was quantified by amplification of the luciferase fragment and normalization to β-globin DNA.

Immunofluorescence Analyses. Cells were fixed in 4% (wt/vol) paraformaldehyde (Electron Microscopy Services) or −20 °C methanol. After washing and blocking in 0.1% donkey serum/0.1% Triton X- 100 in PBS, cells were incubated in primary antibodies overnight at 4 °C (mouse or rabbit anti-human albumin (Sigma Aldrich); goat anti-human α-1-antitrypsin (Bethyl Laboratories); mouse or rabbit anti-human cytokeratin 18 (Sigma Aldrich); rabbit anti-human α-fetoprotein (Santa Cruz); mouse anti-human SOX17 (R&D Systems); goat anti-human HNF4α (Santa Cruz); polyclonal rabbit anti-HBV Core (generously provided by Y. Shaul, The Weizmann Institute, Rehovot, Israel) (7). Secondary antibodies were donkey anti-mouse DyLight 594, donkey anti-rabbit DyLight 488, donkey anti-mouse DyLight 488, or donkey anti-rabbit DyLight 594 conjugates (Jackson Immunoresearch). Cells were counterstained with Hoechst dye (Invitrogen).

Western Blot Analysis of NTCP. Total protein was extracted with radioimmunoprecipitation assay lysis buffer, and samples were separated by electrophoresis on 12% (wt/vol) polyacrylamide gels and electrophoretically transferred to a PVDF membrane (Bio-Rad Laboratories). Blots were probed with NTCP antibody (Aviva Biosystems) followed by HRP-conjugated anti-rabbit secondary antibodies (Amersham), and developed using Super-Signal West Pico substrate (Thermo Scientific).

Albumin and Transferrin ELISA. Media samples were stored at −20 °C. Transferrin and albumin concentrations were measured by sandwich ELISA using HRP detection (Bethyl Laboratories) and 3,3′,5,5′-tetramethylbenzidine (Thermo Scientific) substrate.

Generation of an NTCP-Expressing HepG2 Cell Line. HepG2 cells (p25) in collagen-coated six-well plates were transduced with VSV-G pseudotyped TRIP-based lentiviral pseudoparticles expressing FLAG-hNTCP1-GFP. Transduced cells were expanded to a P100 plate then scaled to a T175 flask. Transduction efficiency was confirmed by flow-cytometry. GFP$^+$ cells were sorted by FACS to intermediate and high GFP$^+$ populations. Intermediate and high GFP-expressing cells were singly sorted in 3× collagen-coated 96-well flat-bottom plates and monitored for growth under the microscope. Multiple clones were tested for HBV infection permissiveness, with clone 3E8 demonstrating the highest infectivity.

1. Schwartz RE, Fleming HE, Khetani SR, Bhatia SN (2014) Pluripotent stem cell-derived hepatocyte-like cells. *Biotechnol Adv* 32(2):504–513.
2. Khetani SR, Bhatia SN (2008) Microscale culture of human liver cells for drug development. *Nat Biotechnol* 26(1):120–126.
3. Langley DR, et al. (2007) Inhibition of hepatitis B virus polymerase by entecavir. *J Virol* 81(8):3992–4001.
4. Yan H, et al. (2012) Sodium taurocholate cotransporting polypeptide is a functional receptor for human hepatitis B and D virus. *eLife* 1:e00049.
5. Glebe D, et al. (2003) Pre-s1 antigen-dependent infection of Tupaia hepatocyte cultures with human hepatitis B virus. *J Virol* 77(17):9511–9521.
6. Shlomai A, Paran N, Shaul Y (2006) PGC-1α controls hepatitis B virus through nutritional signals. *Proc Natl Acad Sci USA* 103(43):16003–16008.
7. Cooper A, Shaul Y (2005) Recombinant viral capsids as an efficient vehicle of oligonucleotide delivery into cells. *Biochem Biophys Res Commun* 327(4):1094–1099.

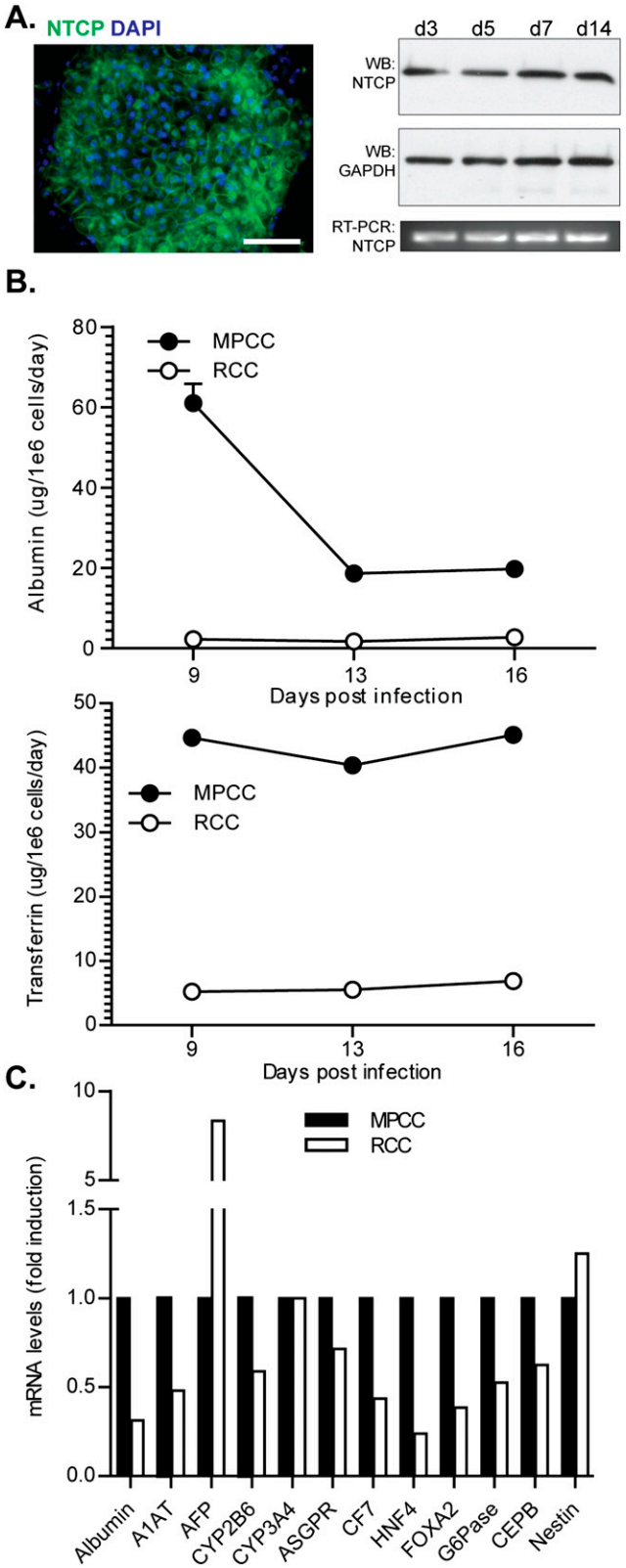

Fig. S1. MPCCs maintain hepatocyte-specific function compared with RCCs. (*A*, *Left*) Immunofluorescence (IF) staining of NTCP shows receptor expression only in circular hepatocyte islands. (Scale bar, 100 μm.) (*Right*) Western blotting and RT-PCR for NTCP protein and RNA, respectively, show receptor maintenance over at least 2 wk. (*B*) MPCCs and RCC hepatocytes (HD4) were analyzed for albumin (*Upper*) and transferrin (*Lower*) levels at the indicated time points after infection with HBV (infection was done 2 d after plating the cells); data expressed as mean ± SEM with $n = 3$. (*C*) MPCCs and RCCs were collected and analyzed for the expression of major genes implicated in normal hepatocyte function, with Janus kinase inhibitor (JAKi) treatment administered to mimic infection conditions.

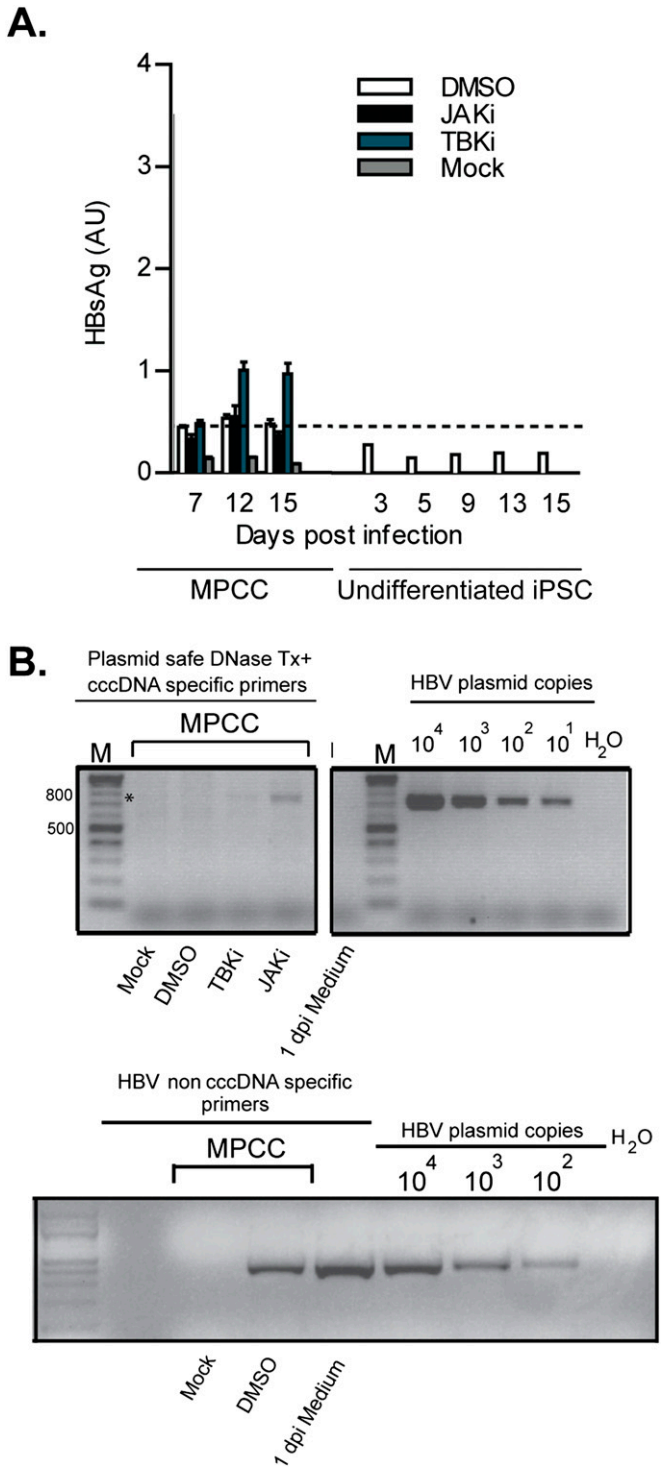

Fig. S2. JAK or TANK binding kinase 1 (TBK1) inhibition enhances HBV infection. (*A*) Primary human hepatocytes (MPCCs) were pretreated with DMSO, JAK, or TBK1 inhibitors 24 h before infection and every other day thereafter. Following incubation with HBV^+ serum for 24 h, medium was collected at the indicated time points for HBsAg analysis (data expressed as mean ± SEM, $n = 3$). iPSCs (nonpermissive for HBV) were used as negative controls. Dotted line indicates the cut-off. (*B*) DNA extracted from HBV-infected cells was amplified using cccDNA-specific primers or primers capable of amplifying all HBV DNA forms following treatment with plasmid-safe DNase, as detailed in *SI Materials and Methods*. PCR products were separated by agarose gel electrophoresis. Two-times HBV plasmid DNA, at the indicated genome equivalents, was used as a positive control. Medium from infected cells 1 day postinfection (dpi) was used as a negative control to show the specificity for cccDNA amplification.

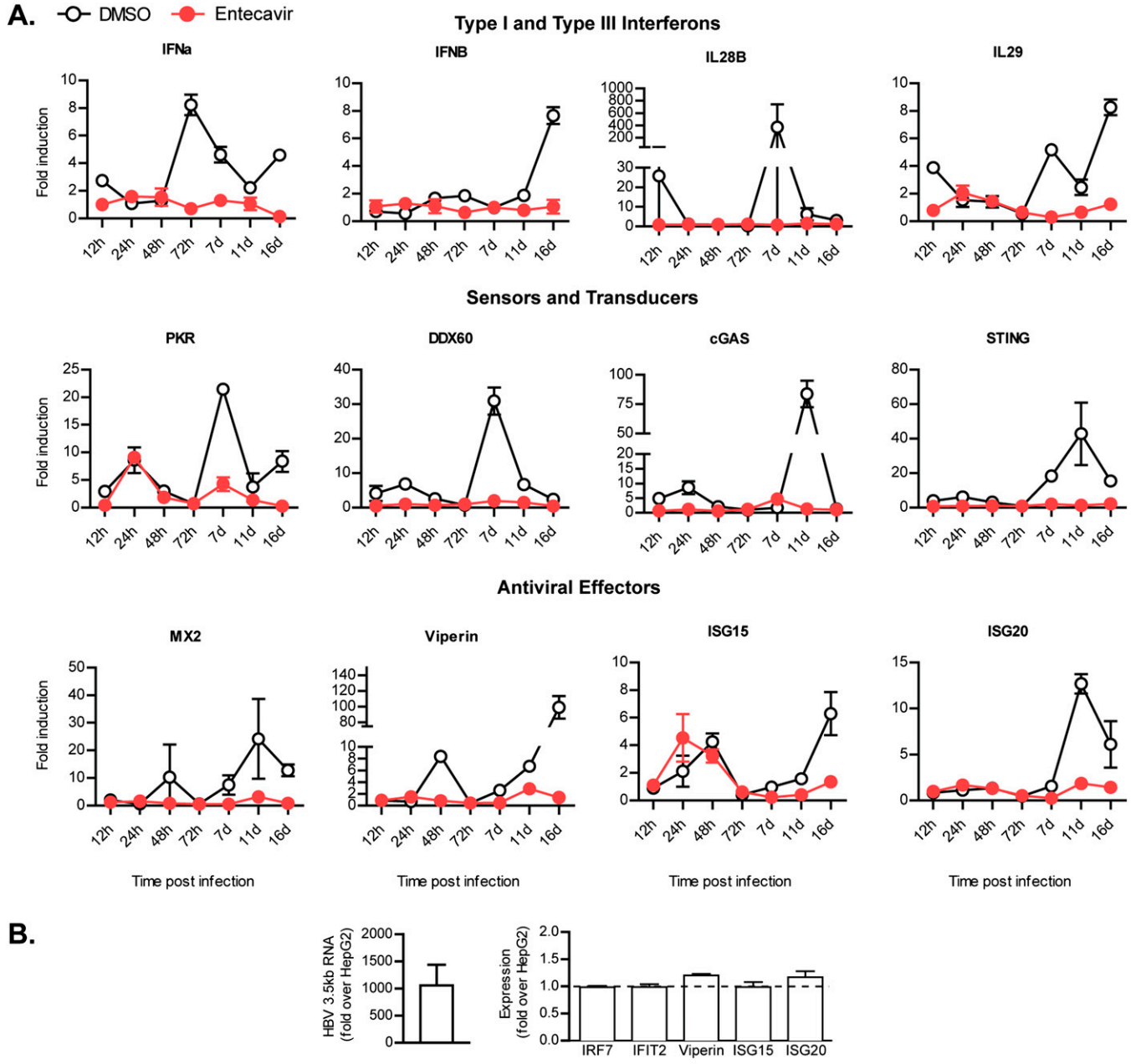

Fig. S3. HBV infection-dependent induction of interferon-stimulated genes (ISGs). (*A*) HD4-derived MPCCs were either mock- or HBV-infected and treated with the reverse-transcriptase inhibitor entecavir or DMSO (vehicle control). Cells were harvested at the indicated times postinfection and RNA was analyzed for the indicated ISGs. Results are normalized to β-actin (and verified with GAPDH) and reported as expression levels relative to the mock-infected cells for each time point. The experiment was done in triplicate and the numbers reflect the mean ± SEM. (*B*) HBV-infected naïve or human NTCP-expressing HepG2 cells were analyzed for 3.5-kb mRNA (*Left*) and ISG RNA expression levels at 9 dpi (*Right*). Results are reported relative to nonpermissive, naïve HBV-infected HepG2 cells ($n = 2$).

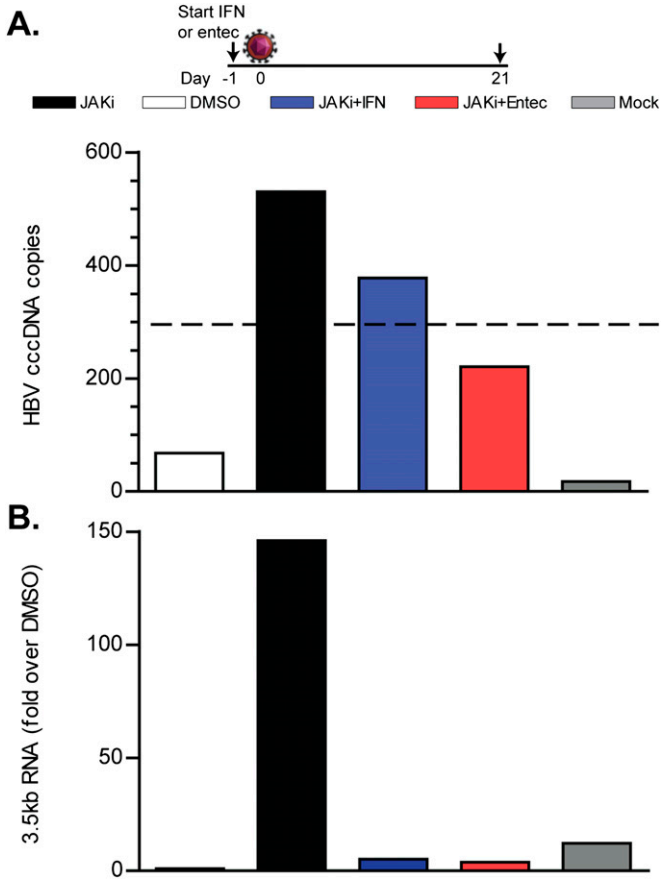

Fig. S4. Prophylactic drug treatment of MPCCs suppresses HBV infection. MPCCs were treated with DMSO (vehicle), JAKi, JAKi and entecavir, or JAKi and IFN-β starting at 1 d before infection. Cultures were subsequently incubated with infectious HBV serum for 24 h. (*A*) At 21 dpi, cell pellets were analyzed for HBV cccDNA (total copies per pellet). Limit of quantification (dotted line). (*B*) Cell pellets analyzed for HBV 3.5-kb mRNA (expression levels relative to HBV infected DMSO treated cells, one pellet per condition per experiment; convergent results were obtained in two independent experiments).

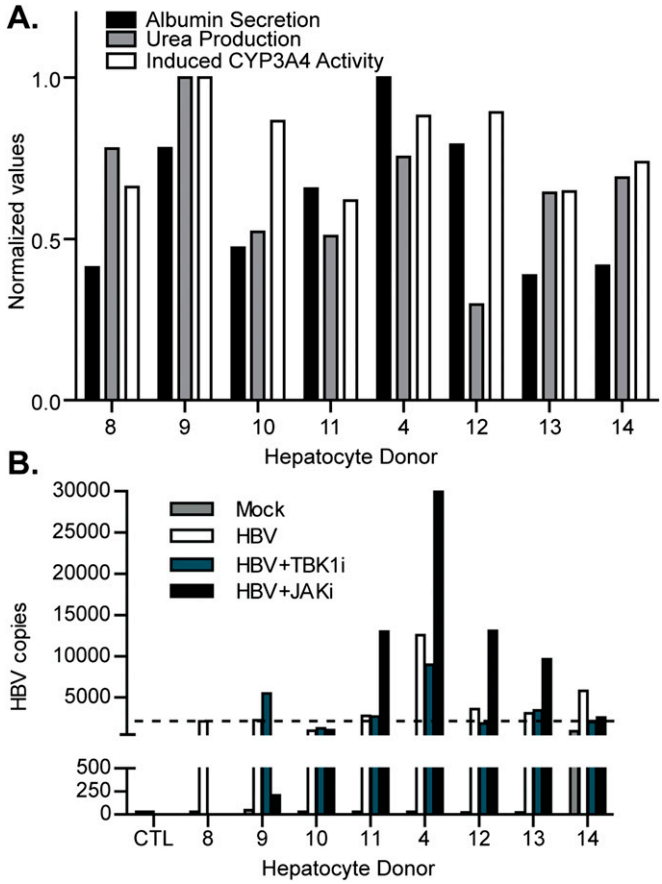

Fig. S5. Common markers of hepatocyte function do not predict donor permissiveness. (*A*) Hepatocytes screened for their HBV permissiveness were also tested for major hepatocyte functions (i.e., albumin secretion, urea production and induced CYP3A4 activity). The set of hepatocyte donors in this experiment is nonoverlapping with the set from Fig. 3, except for HD4, which was used for the majority of experiments in this study. A comparison is presented with the value of 1 representing the most robust activity observed for each of the analyzed parameters. (*B*) MPCCs created with hepatocytes from the donors in *A* were pretreated with DMSO, JAKi, or TBK1i, and infected with HBV. At 16 dpi, cell pellets were harvested and total HBV DNA was extracted and quantified. Limit of quantification (dotted line).

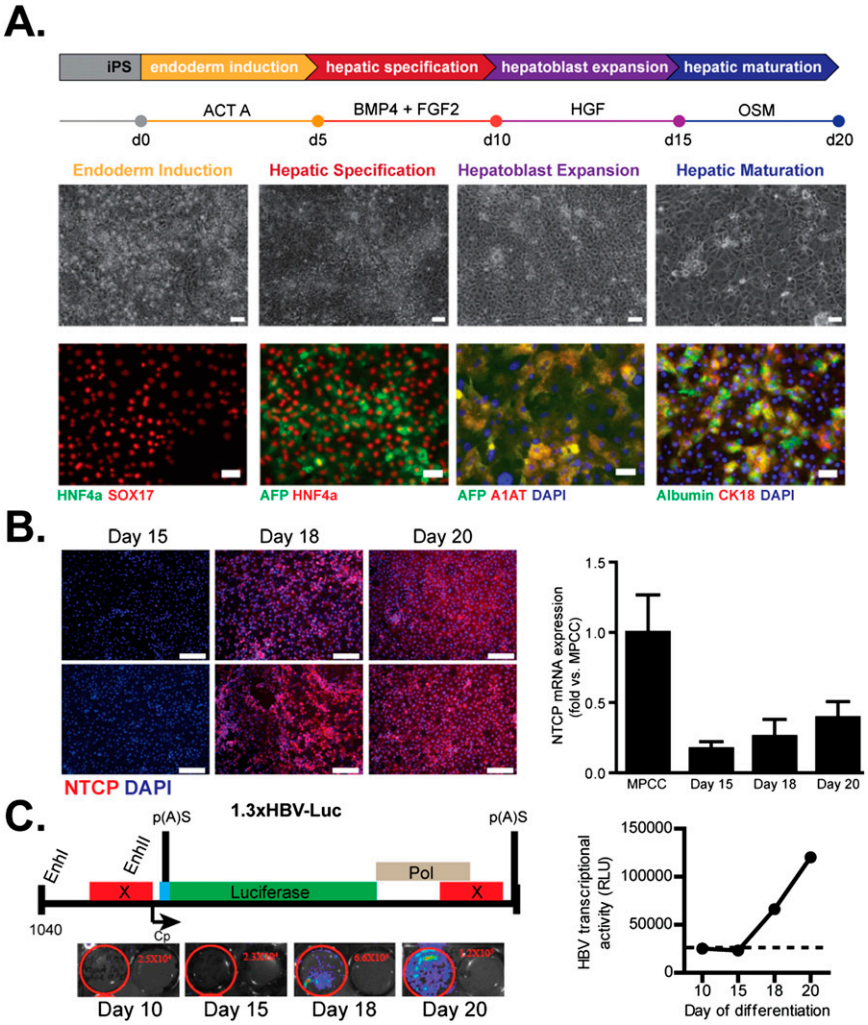

Fig. S6. Expression of NTCP and activation of HBV transcription during iPSC differentiation to iHeps. (*A*, *Upper*) Schematic representation of the stages of differentiation, including cell-culture medium additives used to stimulate the progression to each new stage. (*Lower*) Bright-field microscopy of cellular morphology (*Upper Row*) and immunofluorescence microscopy (*Lower Row*) of stage-specific markers expressed by iPSC-derived cells during differentiation steps. Albumin and CK18 double-positive cells are the most functional iHeps, corresponding to a fetal-like hepatocyte phenotype. (Scale bar, 50 μm.) (*B*) iPSCs were differentiated in a stepwise fashion and immunofluorescent staining for NTCP (two representative examples of each time point are pictured) (*Left*), as well as qRT-PCR for NTCP mRNA (*Right*; $n = 3$ expressed as mean ± SEM) were performed at day 15 (hepatoblast), day 18 (early hepatocyte-like cells), and day 20 (hepatocyte-like cells). (Scale bars, 100 μm.) (*C*) iPSCs were differentiated in a stepwise fashion and transfected with an HBV-luciferase reporter construct (*Upper Left*). Cells were visualized in six-well plates by IVIS imaging (*Lower Left*) and luminescent intensity was measured 72–96 h posttransfection (*Right*). Luminescence intensity is reported as radiance (photons per s/cm^2 per steradian). Dotted line, background luminescence. Data are shown from one representative experiment of three independent replicates yielding similar results.

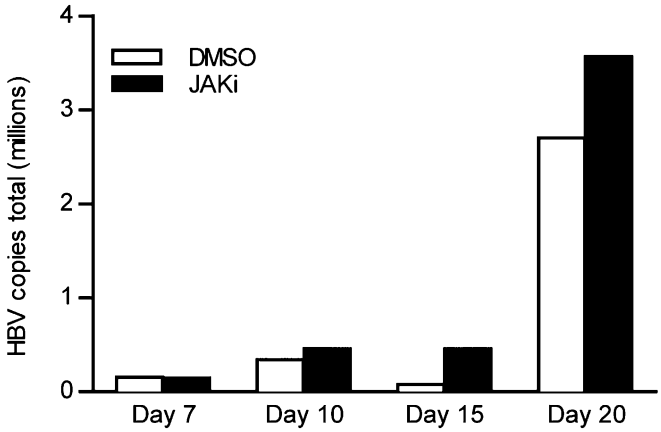

Fig. S7. Analysis of intracellular HBV DNA in iHeps. iPSCs were differentiated and incubated with HBV infectious serum at day 7, day 10, day 15, or day 20 of the differentiation protocol concomitant with treatment with either DMSO (vehicle control) or JAKi. DNA was extracted at day 16 postinfection, and quantified by qPCR (one pellet per condition per experiment, confirmed in two independent experiments).

Table S1. Basic identifying parameters of the hepatocyte donors screened for HBV permissiveness in this study

Lot number	Vendor	Lot	Race	Sex	Age
Donor information for Fig. 3					
HD1	Celsis	OFA		Female	78
HD2	Celsis	TSM		Female	49
HD3	TRL	HUM4012	Caucasian	Male	54
HD5	TRL	HUM4037	Caucasian	Male	8
HD6	TRL	HUM4038	Caucasian	Female	33
HD7	TRL	HUM4040	Caucasian	Female	23
HD4	Celsis	NON		Female	35
Donor information for Fig. S5					
HD8	VWR	8148	Caucasian	Female	55
HD9	VWR	4244	Caucasian	Male	3
HD10	Celsis	BHL		Male	28
HD11	Celsis	IZT		Female	44
HD4	Celsis	NON		Female	35
HD12	Celsis	TRZ		Female	35
HD13	Celsis	YEM		Female	46
HD14	Celsis	YJM		Female	47